VOL. 12, NO. 10, MAY 2017 ISSN 1819-6608
ARPN Journal of Engineering and Applied Sciences

www.arpnjournals.com

TRANSVERSE VORTEXINDUCED VIBRATION OF SPRING-SUPPORTED CIRCULAR CYLINDER WITH MASS RATIO OF 10 TRANSLATING CLOSE TO A PLANE WALL

Meng-Hsuan Chung
Department of Naval Architecture and Ocean Engineering, National Kaohsiung Marine University, Taiwan, ROC
E-Mail: mhsuan@mail.nkmu.edu.tw

ABSTRACT

Transverse vortex induced vibration of a spring-supported circular cylinder with mass ratio of 10 and zero damping translating near a plane wall at Re = 100 is numerically studied. The author investigates three gap ratios. Results show that the size of lock-in zone increases and the peak vibration amplitude decreases with decreasing gap ratio. The peak vibration amplitude occurs at a larger reduced velocity for a smaller gap ratio. The cylinder vibration in the lock-in zone is controlled by either the Strouhal frequency or the natural structure frequency in fluid, depending on the gap ratio and reduced velocity. The time-mean drag in the lock-in zone is always larger than that for an isolated non-vibrating (purely translating) cylinder. The time-mean lift is always positive.

Keywords: vortex induced vibration, translating circular cylinder, plane wall, gap ratio, and cartesian grid method.

INTRODUCTION

Uniform flow over a stationary circular cylinder has attracted much interest among researchers. Vortex shedding in the wake of the circular cylinder frequently occurs and causes periodic forcing to the cylinder. If the cylinder is allowed to vibrate freely in the flow, the vortex shedding and the cylinder motion will influence each other, eventually reaching a state of balanced vibration, called vortex induced vibration (VIV). The term "lock-in" denotes the occurrence of large vibration amplitude in VIV.

VIV of an isolated circular cylinder, rigid or flexible, has been studied extensively in the literature. The parameters involved are the mass ratio m^*(= m/m_d), damping ratio ζ (= c/c_{crit}), reduced velocity U^* (= $U/f_{nw}D$), and Re (= UD/ν) where m = cylinder mass, m_d = displaced fluid mass, c = structural damping, c_{crit}=critical damping,U = free-stream velocity, f_{nw}= natural structure frequency in fluid, D = cylinder diameter, and ν= kinematic viscosity. Much of the related research was reviewed by Sarpkaya [1] and Williamson and Govardhan [2]?.Williamson and Govardhan [3] briefly summarized fundamental results and discoveries related to VIV with very low mass-damping product, $m^*\zeta$. Al Jamal and Dalton [4] reviewed some numerical studies on VIV of a circular cylinder.

The characteristics of the lock-in zone and the wake vortex structure would change significantly when the cylinder is close to a plane wall. For the scenario of VIV near a fixed plane wall in a free stream, two additional parameters have to be considered for this problem. The first is the gap ratio, G, defined as the distance between the wall-side cylinder shoulder and the wall in the static equilibrium condition (i.e., when the spring force keeps zero with quiescent ambient fluid) normalized by D. The second is the wall boundary layer profile. Tsahalis and Jones [5], Jacobsen *et al.* [6], Tofrum and Anand [7] found that the presence of a plane boundary lowers the vibration amplitude. However, Yang *et al.* [8] reported that the vibration amplitude increases with decreasing gap ratio. Raghavan *et al.* [9] indicated that the vibration amplitude as function of gap ratio depends strongly on the Reynolds number and the wall boundary layer. Therefore, the correlation between the vibration amplitude and the gap ratio is still unclear due to insufficient exploration of these influential factors. On the other hand, the vibration frequency as a function of the reduced velocity also differs among various studies [9. 10]. Both Zhao and Cheng [11] and Wang *et al.* [12] reported significant vibration amplitudes even if G= 0.05, in contrast to the case of a stationary cylinder that vortex shedding is suppressed when G< 0.3.

In the present work, the author studies by computational fluid dynamics techniques the 1-dof VIV of a transversely spring-supported zero-damping circular cylinder which is translating near a fixed plane wall with Re = 100. For numerical computations, the original scenario is replaced by an equivalent one where a uniform flow with the translating velocity passes a fixed cylinder above a plane wall which is moving with the same translating velocity. The effect of wall boundary layer thus can be separated out. All the quantities in this work are made dimensionless by taking D, U, and ρ_f(fluid density) as the characteristic length, velocity, and density respectively. Figure-1 depicts the configuration of the physical problem, computational domain, and boundary conditions.

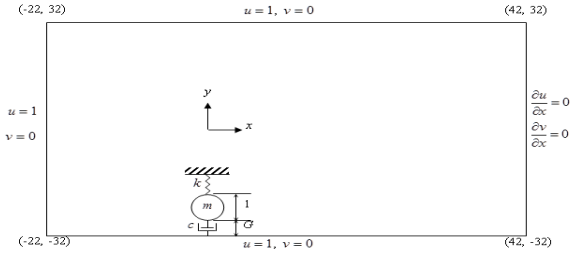

Figure-1. Schematic diagram of the physical problem, computational domain, and boundary conditions.

METHODOLOGY

Fluid flow solver

The Cartesian grid method with a cut cell approach [13] was selected to solve the coupled continuity and Navier-Stokes equations for two-dimensional incompressible flows. It is characterized by a cell-centered collocated finite volume Cartesian grid with AMR (Adaptive Mesh Refinement). The method is nominally second-order accurate in both time and space.

Fluid-solid interaction

The cylinder is rigid, streamwise-fixed, and transversely supported by linear springs with uniform structural damping. A fluid-solid interaction is therefore involved in this physical problem. The dimensionless equation of motion for the 1-dof motion of the circular cylinder is

$$m\ddot{y}_c + c\dot{y}_c + ky_c = F_{y,\text{hydro}} \tag{1}$$

where y_c denotes the coordinate of the centroid of the cylinder in the transverse direction relative to the static equilibrium position and the dot symbol represents the time derivative. The cylinder, which has mass m, is supported by a spring of constant stiffness k. The uniform structural damping of the supporting system is c. The ambient fluid exerts the transverse hydrodynamic force $F_{y,\text{hydro}}$ to the cylinder. The trapezoidal method, which is a classical second-order implicit method, was used to integrate the equations of motion.

Structural parameters

A mass-spring-damper system is usually characterized by another set of three parameters: mass ratio, m^*, natural structure frequency in fluid, f_{nw}, and damping ratio, ζ. Their definitions are

$$m^* \equiv \frac{m}{m_d}, \tag{2}$$

$$f_{nw} \equiv \frac{1}{2\pi}\sqrt{\frac{k}{m+m_A}} \tag{3}$$

$$\zeta \equiv \frac{c}{c_{crit}} \quad \left(c_{crit} \equiv 2\sqrt{k\left(m+m_A\right)}\right). \tag{4}$$

From the definition of reduced velocity,

$$U^* \equiv \frac{U}{f_{nw}D}, \tag{5}$$

we can obtain $U^* = 1 / f_{nw}$ as a result of the present procedure of nondimensionalization. Therefore,

$$m = m^* \cdot m_d, \tag{6}$$

$$k = \left(m+m_A\right)\left(\frac{2\pi}{U^*}\right)^2, \tag{7}$$

$$c = 4\pi\frac{\left(m+m_A\right)\zeta}{U^*} \tag{8}$$

where m_A is the nominal added mass simply set to m_d.

Cylinder impact with wall

The cylinder occasionally hits the wall, causing the cylinder to bounce back. The author assumed that the bounce-back is fully elastic and changes only the vertical velocity of the cylinder. That is, $V_c = -V_c'$ where V_c' and V_c are the vertical velocities of the cylinder before and after bouncing back, respectively. The bouncing back process is completed in one time step. To avoid numerical difficulties, the bouncing back must be actuated when the gap between the cylinder bottom and the wall is smaller than 0.02. Similar treatments were used by Zhao and Cheng [11].

RESULTS AND DISCUSSIONS

Introduced below are a number of physical quantities in terms of which the results will be presented. The maximal and minimal amplitudes of the vertical displacement, $A_{\max}$ and $A_{\min}$, are defined as the maximum and minimum among all local amplitudes, respectively. The predominant frequency of cylinder vibration, f_{cyl}, is defined as the average of all the local frequencies. The phase lag, ϕ, is defined as the phase lag of the oscillation of the vertical displacement behind that of the lift force. The drag and lift coefficients are defined as

$$C_{\text{D}} = \frac{2F_{x,\text{hydro}}}{\rho U^2 D} \quad \text{and} \quad C_{\text{L}} = \frac{2F_{y,\text{hydro}}}{\rho U^2 D} \tag{9}$$

where $F_{x,\text{hydro}}$ and $F_{y,\text{hydro}}$ are respectively the streamwise and transverse hydrodynamic forces exerted on the cylinder surface by the ambient fluid. The quantities $C_{\text{D,mean}}$, and $C_{\text{L,mean}}$ denote the corresponding time-mean values of C_{D} and C_{L}. Finally, f_{L} denotes respectively the predominant frequency and the amplitude of the lift coefficient variation. The Strouhal frequency, f_0, denotes the dimensionless frequency of vortex shedding for a stationary isolated circular cylinder.

The origin of the coordinate system is the static equilibrium position of the cylinder center. The initial position of the cylinder center is (0, 0.02) to rapidly trigger the alternative vortex shedding. The computational domain [-22, 42]×[-32, 32] was used with the smallest mesh size of 1/128 clustered near around the cylinder surface.

To validate the present method, the author performed simulations with Re = 200, m^* = 10, and ζ = 0.01, the same as used in [14] and [15]. As shown in Figure-2, the present prediction of the peak of $A_{\max}$, 0.5, is nearly the same as that of [14] and both results exhibit the

phenomenon of a sharp decrease of A_{max} at the upper end of the lock-in zone. The peak value of A_{max} occurs near the lower end of the lock-in zone in each study. All the three result are consistent with each other.

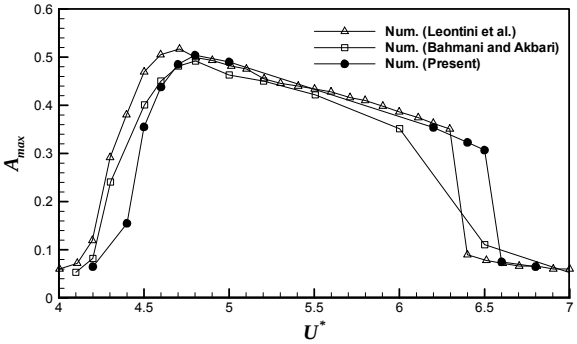

Figure-2. Variation of A_{max} with U^* for an isolated cylinder with $m^* = 10$, $\zeta = 0.01$, Re = 200. Also shown are results from previous contributions.

Near-wall cases

With $m^* = 10$ and $\zeta = 0$, the author examined the effects of the gap ratio on various aspects of hydrodynamic and structural responses, including their interactions, by setting $G = 0.06$, 0.3, and 31.5. The cases with $G = 31.5$ can be regarded as for an isolated cylinder. The Reynolds number was fixed at 100.

For each gap ratio, the author performed a series of simulations with varied reduced velocities ($3 \le U^* \le 10$). Figure-3 shows the variation of A_{max} and A_{min} with U^* for the three gap ratios. The sizes of the lock-in zone are approximately $5 \le U^* \le 7.5$ and $3.5 \le U^* \le 7.5$ for $G = 31.5$ and 0.3 respectively, i.e., increasing with decreasing gap ratio. There does not exist a lock-in zone for $G = 0.06$ due to too small vibration amplitudes. The gap ratio has a strong influence on the peak of A_{max}, which decreases to 0.06 with the gap ratio decreasing to 0.06. The onset of lock-in occurs at lower reduced velocities than for an isolated cylinder. The reduced velocity where A_{max} occurs, U^*_{peak}, increases with decreasing gap ratio and the rate at which A_{max} changes with U^* near the two ends of the lock-in zone is slower for a smaller gap ratio. The phenomenon well known for an isolated cylinder with high-mass ratio is reconfirmed in this study: the rate of A_{max} varying with U^* near the onset of the lock-in zone exceeds that near the upper end of the lock-in zone. However, this characteristic disappears when the VIV occurs near a moving wall. Conversely, the rate of A_{max} varying with U^* near the lower end is smaller than that near the upper end of the lock-in zone for $G = 0.3$. In most cases A_{min} follows exactly the same curve as that of A_{max}. The only two exceptions occur at $U^* = 5$ and 8 for $G = 31.5$ which are caused by the beating-like phenomena in the unshown time history of y_c. The cylinder vibration thus exhibits strong regularity in the lock-in zone.

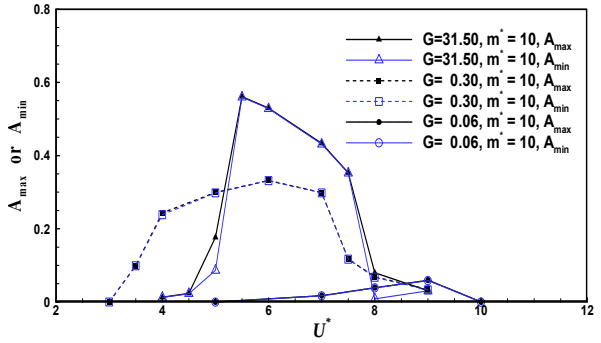

Figure-3. Variation of A_{max} and A_{min} for three gap ratios.

Figure-4 shows the variation of f_{cyl}/f_{nw} and f_L/f_{nw} with U^* for the three gap ratios, in comparison with the straight line representing the Strouhal frequency at Re = 100. For all the three gap ratios, the author finds that $f_{cyl} = f_L$ in the whole range of U^* studied ($3 \le U^* \le 10$). $f_{cyl} \approx f_L \approx f_{nw}$ throughout the lock-in zone, if any. This is consistent with many previous results indicating that the vibration frequency of a high-mass-ratio cylinder tends to be close to the natural structure frequency in fluid. The frequency ratio at U^*_{peak} exceeds 1 for each gap ratio and increases with decreasing gap ratio.

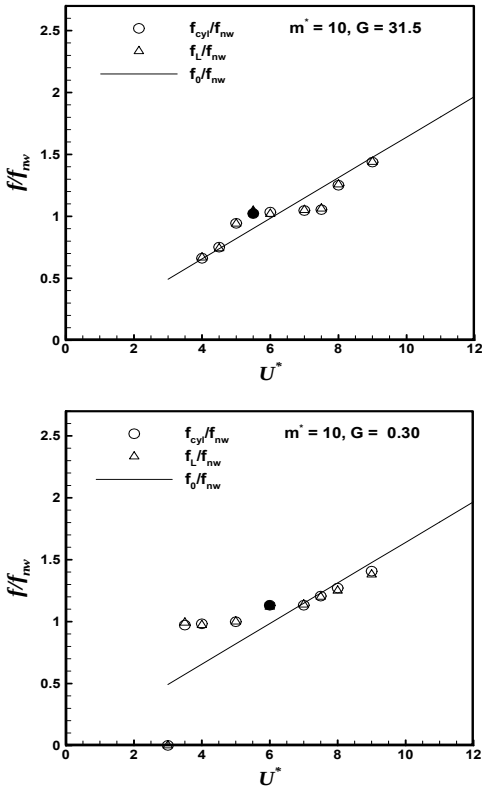

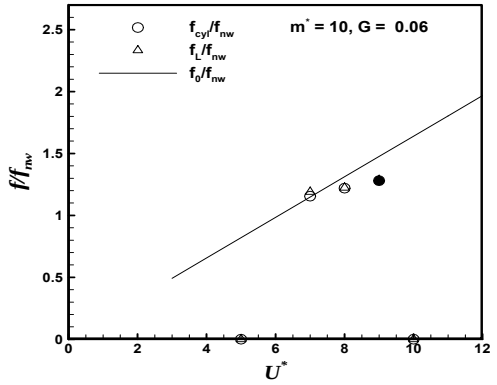

Figure-4. Variation of f_{cyl}/f_{nw} and f_L/f_{nw} with U^* for three gap ratios. Solid symbol: occurrence of the peak of A_{max}.

Figure-5 shows the average phase lag, ϕ, of the cylinder response behind the hydrodynamic lift. For an isolated cylinder, the phase lag exhibits a sharp jump from approximately 0° to 180° at U^* between 7 and 7.5 and remains at 0° and 180° for a lower and higher reduced velocity, respectively. For G = 0.3, the phase lag jump is slightly smoother than that for an isolated cylinder and followed by an overshoot-undershoot variation. For G = 0.06, the phase lag remains nearly constant at 200°. For each gap ratio, the jump area ends at a reduced velocity larger than U^*_{peak}.

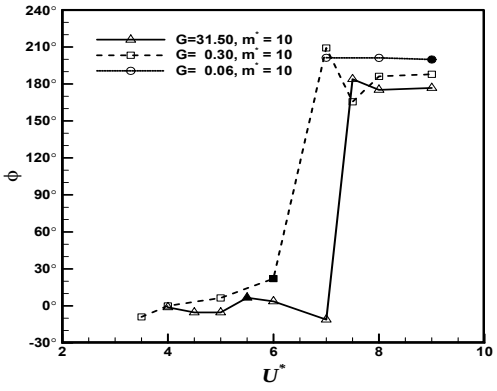

Figure-5. Variation of ϕ with U^* for three gap ratios. Solid symbol: occurrence of the peak of A_{max}.

Figure-6 shows the variation of $C_{D,mean}$ with U^* for the three gap ratios. The time-mean drag is larger than that for an isolated fixed cylinder in all cases except those for G = 31.5 with reduced velocities higher than the upperend of the lock-in zone; the maximal $C_{D,mean}$ occurs at or not far from U^*_{peak} for those gap ratios exhibiting significant vibration amplitudes, G = 31.5 and 0.3. The maximal $C_{D,mean}$ differs significantly among the three gap ratios and peaks for an isolated cylinder. Also shown in Figure-6 are the variations of $C_{L,mean}$ with U^*. The time-mean lift is always positive and the small-gap-ratio cylinder acquires a higher time-mean lift than the large-gap-ratio cylinder in the entire range of reduced velocity.

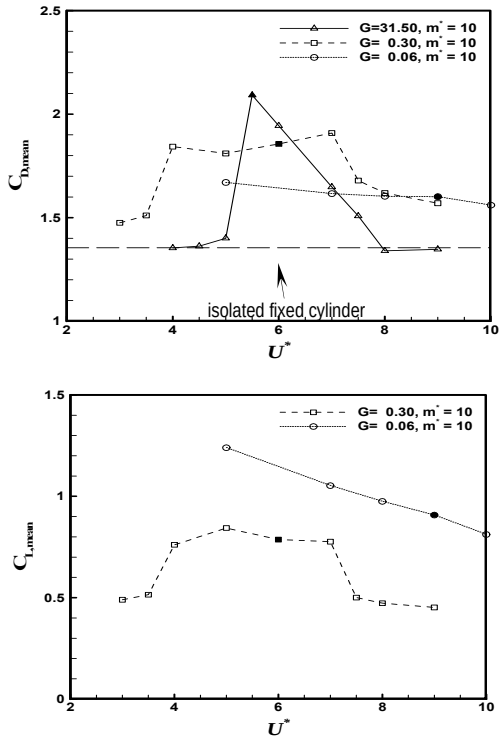

Figure-6. Variation of $C_{D,mean}$ and $C_{L,mean}$ with U^* for three gap ratios. Solid symbol: occurrence of the peak of A_{max}.

CONCLUSIONS

The characteristics of 1-dof VIV of a zero-damping circular cylinder with the mass ratio of 10 near a moving wall at Re = 100 was numerically examined in this study. The major findings and conclusions are collected as below.

The peak vibration amplitude decreases significantly with decreasing gap ratio. With decreasing gap ratio, both the onset smoothness and size of the lock-in zone increases and the onset of lock-in occurs at lower reduced velocities. The steep-rise-and-soft-decline profile characteristic of high-mass-ratio VIV for an isolated cylinder disappears while approaching a moving wall. The local amplitude of vibration hardly changes with time.

The predominant vibration frequency is always equal to the predominant lift frequency, which is close to the natural structure frequency in fluid in the lock-in zone. For a cylinder near the wall, the phase lag jump is slightly smoother than that for an isolated cylinder.

The time-mean drag is larger than that for an isolated fixed circular cylinder in the lock-in zone for all cases investigated in this study. The maximal time-mean drag changes significantly and occurs at a higher reduced velocity as the gap ratio decreases. The time-mean lift is always positive for all near-wall cases investigated in this study. A smaller gap ratio causes a higher time-mean lift at a given reduced velocity.

REFERENCES

[1] Sarpkaya T. 2004. A critical review of the intrinsic nature of vortex-induced vibrations. Journal of Fluids and Structures. 19: 389-447.

[2] Williamson C. H. K. and Govardhan R. 2004. Vortex-induced vibrations. Annual Review of Fluid Mechanics. 36: 413-455.

[3] Williamson C. H. K. and Govardhan R. 2008. A brief review of recent results in vortex-induced vibrations. Journal of Wind Engineering and Industrial Aerodynamics. 96: 713-735.

[4] Al Jamal H. and Dalton C. 2005. The contrast in phase angles between forced and self-excited oscillations of a circular cylinder. Journal of Fluids and Structures. 20(4 SPEC. ISS.): 467-482.

[5] Tsahalis D. T. and Jones W. T. 1981. Vortex-induced vibrations of a flexible cylinder near a plane boundary in steady flow. Proceedings of the Annual Offshore Technology Conference 1,367-381. Houston, TX. Offshore Technol. Conf., Dallas, TX, USA.

[6] Jacobsen V., Bryndum M. B. and Nielson R. 1984. Cross-flow vibrations of a pipe close to a rigid boundary. ASME Journal of Energy Resources Technology. 106(4): 451-457.

[7] Torum A. and Anand N. M. 1985. Free span vibrations of submarine pipelines in steady flows - effect of free-stream turbulence on mean drag coefficients. ASME Journal of Energy Resources Technology. 107(4): 415-420.

[8] Yang B., Gao F. P., Wu Y. X. and Li D. H. 2006. Experimental study on vortex-induced vibrations of submarine pipeline near seabed boundary in ocean currents. China Ocean Engineering. 20(1): 113-121.

[9] Raghavan K., Bernitsas M. M. and Maroulis D. 2009. Effect of bottom boundary on VIV for energy harnessing at $8\times10^3 < Re < 1.5\times10^5$. ASME Journal of Offshore Mechanics and Arctic Engineering. 131(3), 031102 (13) pages.

[10] Fredsoe J., Sumer B. M., Andersen J. and Hansen E. 1987. Transverse vibrations of a cylinder very close to a plane wall. ASME Journal of Offshore Mechanics and Arctic Engineering. 109(1): 52-60.

[11] Zhao M. and Cheng L. 2011. Numerical simulation of two-degree-of-freedom vortex-induced vibration of a circular cylinder close to a plane boundary. Journal of Fluids and Structures. 27(7): 1097-1110.

[12] Wang X. K., Hao Z. and Tan S. K.2013.Vortex-induced vibrations of a neutrally buoyant circular cylinder near a plane wall. Journal of Fluids and Structures. 39: 188-204.

[13] Chung M-H.2015. Hydrodynamics of flow over a transversely oscillating circular cylinder beneath a free surface. Journal of Fluids and Structures. 54: 27-73.

[14] Leontini J. S., Thompson M. C. and Hourigan K. 2006. The beginning of branching behaviour of vortex-induced vibration during two-dimensional flow. Journal of Fluids and Structures. 22: 857-864.

[15] Bahmani M. H. and Akbari M. H. 2010. Effects of mass and damping ratios on VIV of a circular cylinder. Ocean Engineering. 37: 511-519.